Available online at www.sciencedirect.com

ScienceDirect

Proceedings of the Combustion Institute (2022) 1–11

Proceedings of the Combustion Institute

www.elsevier.com/locate/proci

Strong flame acceleration and detonation limit of hydrogen-oxygen mixture at cryogenic temperature

Xiaobo Shen [a,b,*], Wenju Fu [a], Wenkai Liang [c], Jennifer X. Wen [b,*], Haifeng Liu [d], Chung K. Law [c,e]

[a] School of Resources & Environmental Engineering, East China University of Science and Technology, Shanghai, 200237, China

[b] Warwick FIRE, School of Engineering, University of Warwick, Coventry, CV4 7AL, United Kingdom

[c] Department of Mechanical and Aerospace Engineering, Princeton University, Princeton, NJ 08544, United States

[d] Shanghai Engineering Research Center of Coal Gasification, East China University of Science and Technology, Shanghai 200237, China

[e] Center for Combustion Energy, Tsinghua University, Beijing 100084, China

Received 5 January 2022; accepted 1 July 2022

Abstract

A series of experiments were carried out in a closed tube at cryogenic temperature (77 K) for hydrogen-oxygen mixtures. Flame propagation speed and overpressure were measured by optical fibers and pressure sensors, respectively. The first and second shock waves were captured in the cryogenic experiments, although the shock waves always precede the flames in all cases indicating the absence of stable detonation. However, strong flame acceleration was observed for all situations, which is consistent with the prediction by expansion ratio and Zeldovich number. Besides, the tube diameter and length are also critical for flame acceleration to supersonic. All the flames in this work accelerate drastically reaching the C-J deflagration state. But at 0.4 atm, only fast flame is formed, while at higher initial pressures, the flame further accelerates to a galloping mode manifesting a near-limit detonation, which could be indicated by the stability parameter χ.

Keywords: Hydrogen; Cryogenic temperature; Strong flame acceleration; Fast flame; Galloping mode

1. Introduction

In response to the global call to reduce greenhouse gas emissions, hydrogen is identified as a candidate of carbon-free energy carrier. Furthermore, since liquid hydrogen as compared to gaseous hydrogen, has the additional attraction in terms of transportation and storage. The development of hydrogen liquefaction and storage technology will give rise to a significant increase of usage of liquid hydrogen in aerospace, ground transportation, civil utility and industry. However, there

* Corresponding author.
E-mail address: ustcshenxb@gmail.com (X. Shen).

https://doi.org/10.1016/j.proci.2022.07.005

are safety concerns related to accidental release of cryogenic LH_2 ($CryoLH_2$), which is typically −252.87 °C and below the freezing temperature of oxygen (O_2) (−218.8 °C). $CryoLH_2$ also evaporates with a volume expansion of 1:848, posing significant risk as a highly flammable gas that could lead to the formation of destructive detonation waves.

While extensive studies have been conducted at room temperature on the initiation of detonation, including deflagration to detonation transition (DDT), there have been only a handful of studies at cryogenic initial temperature. At present, the research on cryogenic temperature mainly focuses on the measurement of flammability limits. For example, Karim et al. [1]. investigated the lean flammability limits of hydrogen, methane and carbon monoxide in air at atmosphere pressure under initial temperature down to −130 °C. Cui et al. [2]. found that as the initial temperature decreased the maximum explosion pressure increased significantly. In addition to flammability limits, published research on cryogenic hydrogen release primarily focused on the jet flow and the subsequent jet flame [3–7] by a limited number of groups from Sandia National Laboratory, Japan Aerospace Exploration Agency, Health and Safety Executive (UK), Karlsruhe Institute of Technology (KIT) and Universities of Warwick and Ulster. The gas cloud deflagrations or even detonations in confined space resulted from cryogenic hydrogen leakage were rarely investigated with the only paper by Kuznetsov et al. [8] in the public domain. Kuznetsov et al. [8] investigated flame acceleration (FA) and detonability criterion for smooth and obstructed channels in hydrogen-air mixtures at cryogenic initial temperature. They found that the expansion ratio was the key factor that caused effective FA, and the run-up distance to detonation at cryogenic temperature was several times shorter than at environment temperature.

Due to higher density for hydrogen at cryogenic temperature, the maximum combustion pressure and detonation pressure will be 2–3 times higher (e.g. at 100 K [8]); and in the meantime, as the speed of sound is about 2 times smaller at cryogenic temperature, the corresponding dynamic pressure will also be 2-3 times higher for the same flame velocity at ambient condition, leading to faster flame acceleration (FA) and prone to transit to detonation. Insights of FA in cryogenic conditions are essential for assessing the potential hazards of accidental liquid hydrogen release as well as cryogenic hydrogen combustion and for detonation engines. Research is much needed to address the significant knowledge gaps on this topic.

Recognizing the lack and hence need of understanding on FA and detonation limits in hydrogen-oxygen mixtures at cryogenic temperature, experimental study has been conducted in a tube at the initial cryogenic temperature (T_0) of 77 K. The specifics of the investigation, the scientific rationale, and the results are presented in the following.

2. Experiments

Fig. 1 shows a schematic diagram of experimental apparatus. The premixing system consists of a 6 L gas premixed cylinder, a bottle of oxygen (99.999%) and a bottle of hydrogen (99.9%). A pair of ignition electrodes are installed at one end of tube. The data acquisition system consists of 17 optical fibers, 2 PCB pressure sensors, a Photoelectric converter, an oscilloscope and a computer. The type of oscilloscope is Pico Scope 4824A. The variation in the explosion pressure is recorded by two PCB pressure sensors (PCB 112A03), which have a measuring range of 0–68 MPa with an accuracy of 0.4% of full scale (FS). Flame propagation process in tube can be measured by optical fibers and Photoelectric converter, which can convert the optical signal into the electrical signal and transmit it to an oscilloscope. And more details about distribution of ignition electrodes, optic fibers and PCB pressure sensors on the tube wall are demonstrated in Fig. 2. The explosion cylindrical tube is made of 316 stainless steels. The cooling system consists of explosion cylindrical tube placed into liquid nitrogen to control cryogenic temperature condition (77 K).

The premixed gas was prepared in a 6 L gas premixed cylinder by partial pressure with hydrogen and oxygen, and the premixed cylinder was placed for 24 h to make sure the hydrogen and oxygen mix evenly prior to experiments. At the beginning of the tests, the tube was vacuumized to make the pressure in tube lower than 0.01 psi. Subsequently, the premixture of hydrogen and oxygen was filled into the test tube of 100 cm long until reaching the inflation pressure. Then liquid nitrogen would be poured into a wooden trough until the entire tube was submerged in liquid nitrogen completely. A simple CFD simulation was performed, which indicated that three minutes were enough for the tube and the mixture inside cooling down to 77 K. Therefore, during each experiment, the tube filled with premixed gas would be immersed into the liquid nitrogen for at least six minutes before ignition. To prevent oxygen from liquefying, the vapor pressure of O_2 at 77 K should be less than 2.910 psi.

Please cite this article as: X. Shen, W. Fu, W. Liang et al., Strong flame acceleration and detonation limit of hydrogen-oxygen mixture at cryogenic temperatures, Proceedings of the Combustion Institute, https://doi.org/10.1016/j.proci.2022.07.005

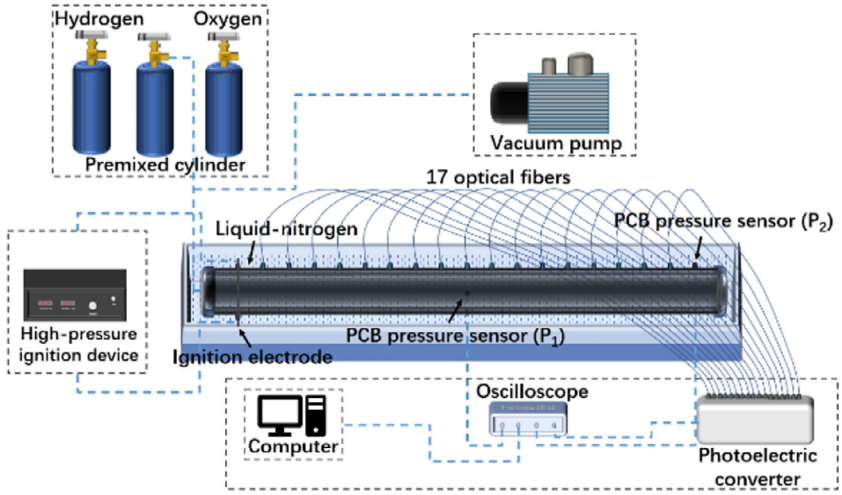

Fig. 1. Schematic diagram of experimental device.

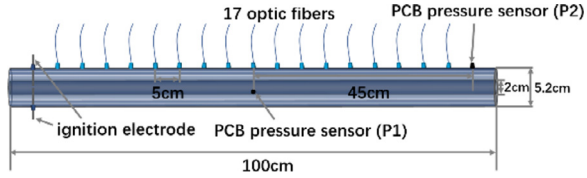

Fig. 2. Schematic diagram of optical fiber and PCB pressure sensors distribution.

Table 1
The experimental conditions of hydrogen-oxygen mixtures.

Initial pressure at 77 K (atm)	Inflation pressure at 298.15 K (psi)	φ	T_0 (K)
0.4	22.717	2.6	77
0.6	34.076	2.6	77
0.8	45.435	2.6	77
1.0	56.793	2.6	77

In the test, an equivalence ratio (φ) of 2.6 was chosen for the hydrogen-oxygen mixture. The experimental conditions are summarized in Table 1.

3. Analytical methods

3.1. C-J detonation parameters

For the aim of analyzing experimental results comprehensively, the C-J detonation parameters are calculated by tangency solutions of Rayleigh Line and Hugoniot Curve, see Table 2. P_0 is the initial pressure at 77 K, V_{cj} is the C-J detonation velocity, P_{cj} is the C-J detonation pressure, and a_p is the sound speed in products.

Table 2
The C-J detonation parameters of hydrogen-oxygen mixtures at 77 K.

P_0 (atm)	V_{cj} (m/s)	P_{cj} (MPa)	a_p (m/s)
0.4	3429.755	2.273	1908.316
0.6	3428.039	3.405	1907.361
0.8	3947.351	6.026	2191.569
1.0	3945.086	7.522	2190.312

3.2. Real-fluid modeling

The laminar flame speed calculations are performed by using the PREMIX code [9] with the kinetic scheme for hydrogen by Burke et al. [10]. The relevant parameters in the later part are calcu-

Please cite this article as: X. Shen, W. Fu, W. Liang et al., Strong flame acceleration and detonation limit of hydrogen-oxygen mixture at cryogenic temperatures, Proceedings of the Combustion Institute, https://doi.org/10.1016/j.proci.2022.07.005

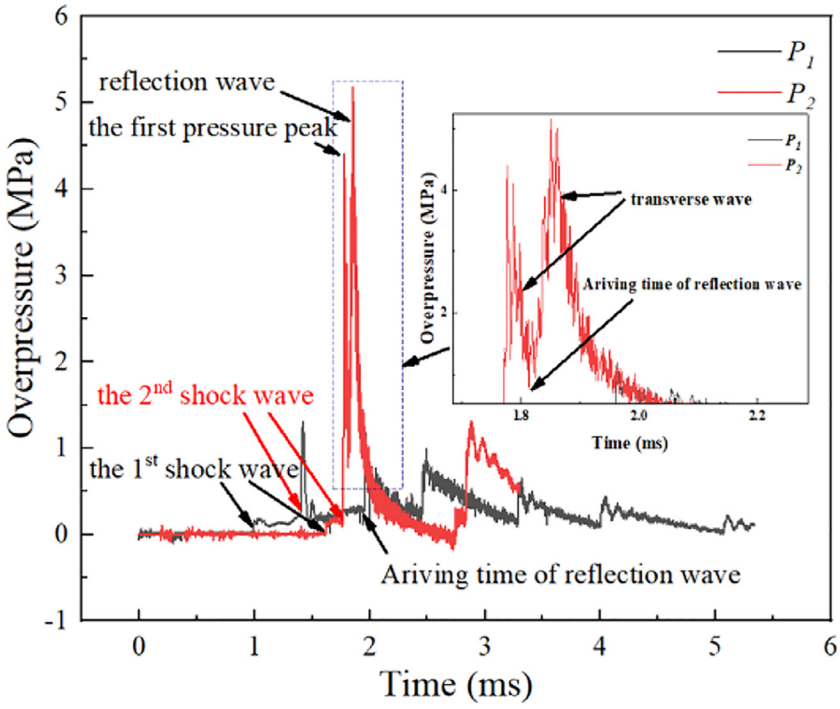

Fig. 3. Pressure profiles of hydrogen-oxygen mixtures at 0.8 atm and 77 K (P_1 and P_2 refer to pressure sensors which are installed in the middle (P_1) and rear (P_2) positions of tube, respectively.).

lated by ANSYS CHEMKIN. To account for the non-ideality of dense fluids, we adopt the Soave-Redlich-Kwong (SRK) equation of state (EoS) [11] to replace the ideal gas law.

To calculate the real-fluid thermodynamic properties, the departure function formulation is used. For example, the specific enthalpy of certain species can be determined as the ideal specific enthalpy plus the departure function:

$$h = h_{ideal} + \frac{1}{W}\left[RT(Z-1) + \frac{T\frac{da}{dT} - a}{b} \times \ln\frac{b+V_m}{V_m}\right] \quad (1)$$

where h_{ideal} is the specific enthalpy of the ideal gas, W is the average molecular weight, and the compressibiliy $Z = PV_m/RT$.

4. Results and discussion

4.1. Flame and shock wave

Fig. 3 shows the pressure profiles of hydrogen-oxygen mixtures at 0.8 atm and 77 K which are measured in the middle (P_1) and rear (P_2) positions of the tube, respectively. The measured pressure traces in both P_1 and P_2 start with a small "step", and then increase to form a peak rapidly. Kellenberger and Ciccarelli [12] found the existence of two discrete shock waves in front of the flame and finally the two discrete waves merged to form a stronger precursor shock wave while investigating the effect of obstacles on detonation wave. They demonstrated that the formation of the second shock wave was caused by the flame tip accelerating through the obstacles. Subsequently, Cheng et al. [13,30] also observed the existence of two discrete shock waves, and showed the 1st shock wave was formed by the combination of a series of weak compression shock waves during flame expansion and the flame tip disturbance in the acceleration stage was responsible for the formation of the 2nd shock wave.

Fig. 4 shows the relationship between the initial pressure and arrival time of the 1st and 2nd shock waves at the middle and end positions of the tube, respectively. As the initial pressure increases, there is a decreasing tendency for the arrival time of both shock waves at different positions. Following the analysis of Cheng et al. [13,32], the 1st shock wave is related to the disturbance in the wrinkled flame surface caused by flame instabilities. Therefore, larger flame instabilities can promote its formation in the early stage of flame expansion.

Table 3 lists the expansion ratio (σ), flame thickness (l_f) and the Markstein length (L_b) at various

Please cite this article as: X. Shen, W. Fu, W. Liang et al., Strong flame acceleration and detonation limit of hydrogen-oxygen mixture at cryogenic temperatures, Proceedings of the Combustion Institute, https://doi.org/10.1016/j.proci.2022.07.005

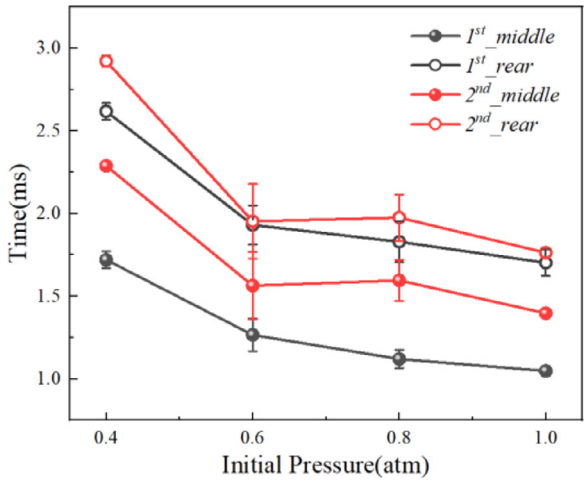

Fig. 4. The relationship between the initial pressure and arrival time of the 1st and 2nd shock waves at the middle and end position of the tube, respectively.

Table 3
The calculated Markstein length (L_b) at different initial pressures and 77 K.

P_0 (atm)	σ	Le_{eff}	β	l_f (cm)	L_b (cm)
0.4	26.81	1.6	8.501	0.0701	0.107
0.6	27.01	1.6	8.476	0.0421	0.064
0.8	27.17	1.6	8.649	0.0295	0.046
1.0	27.26	1.6	8.651	0.0226	0.035

conditions. Le_{eff} is the effective Lewis number [33], and β is the Zeldovich number. L_b is a global flame parameter which quantitatively describes the effect of flame stretch rate on the stretched laminar flame propagation speed (S_b) [14]. Generally, larger L_b represents higher stability of flame. In this work, L_b decreases with initial pressure. The increasing σ and decreasing l_f manifest potential enhancement of hydrodynamic instability of the flame [15]. Therefore, elevated initial pressure can strengthen flame instability and consequently promote earlier formation of the 1st shock wave.

The 2nd shock wave is associated with the flame tip disturbance during FA, which is strongly dependent on the expansion ratio, a larger expansion ratio can strengthen FA to shorten the time required for its formation. Increasing the initial pressure leads to an increase of the expansion ratio, which greatly enhances FA. Thus, elevated initial pressure can also greatly promote earlier formation of the 2nd shock wave. It can be inferred from Fig. 4 that the 2nd shock wave is more sensitive to initial pressure than the 1st one due to the reinforcement of FA.

In addition, with the flame propagating forward, the delay time (t_d) of both shock waves arriving at the middle and end positions of the tube decreases gradually, enabling the 2nd shock wave to catch up with the 1st one. They merge to form a stronger precursor shock wave prior to the onset of detonation. This is consistent with the findings of Cheng et al. [13]. It can be inferred that a longer test tube can facilitate the observation of this phenomenon.

Fig. 5 shows the time for the flame and the two shock waves to reach different positions at 0.4 and 1.0 atm. Both shock waves propagate ahead of the flame, but the distance between them decreases gradually. Thus, the flame and shock waves are decoupled, indicating non-existence of stable detonation.

Fig. 6 shows the peak overpressure profile measured by the two pressure sensors installed in the middle (P_1) and end (P_2) positions of the tube, with the $P_{1\_reflection}$ and $P_{2\_reflection}$ referring to the peak overpressure of the reflected shock wave measured by P_1 and P_2, respectively. None of the measured peak overpressures reach the theoretical C-J detonation values. As the initial pressure increases, the peak overpressures increase for both P_1 and P_2.

Furthermore, the peak overpressure for $P_{2\_reflection}$ is higher than P_2, while that for $P_{1\_reflection}$ is smaller than P_1 at different initial pressures. This is because that P_2 is close to the end wall and suffers a superimposed effect of the shock wave and its reflection from the end wall. The reflected shock wave propagates backwards and attenuates gradually, which explains the reason that the peak overpressure of $P_{1\_reflection}$ is smaller than P_1.

4.2. The critical deflagration state

Fig. 7 shows the flame propagation velocity as function of position at different initial pressures. It is seen that in all cases the flame accelerates to

Please cite this article as: X. Shen, W. Fu, W. Liang et al., Strong flame acceleration and detonation limit of hydrogen-oxygen mixture at cryogenic temperatures, Proceedings of the Combustion Institute, https://doi.org/10.1016/j.proci.2022.07.005

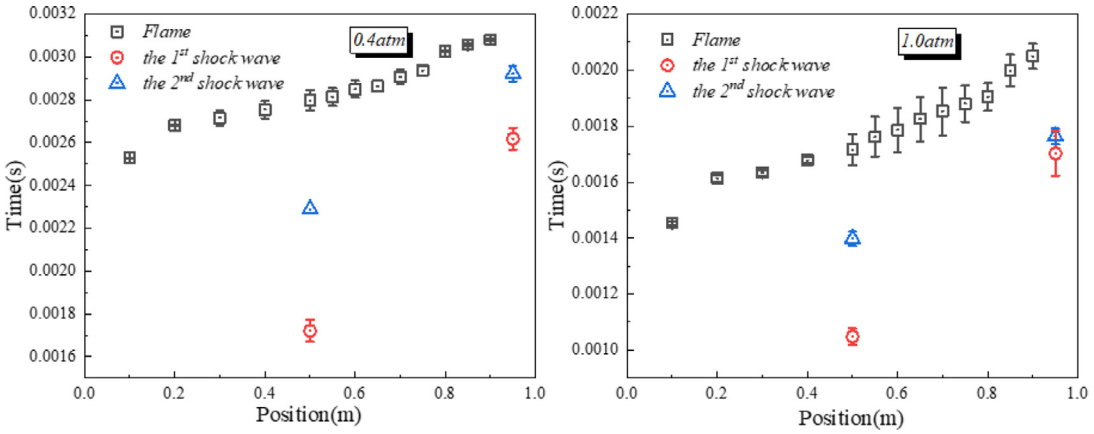

Fig. 5. The time for the flame and the two shock waves to reach different positions as function of position at 0.4 and 1.0 atm.

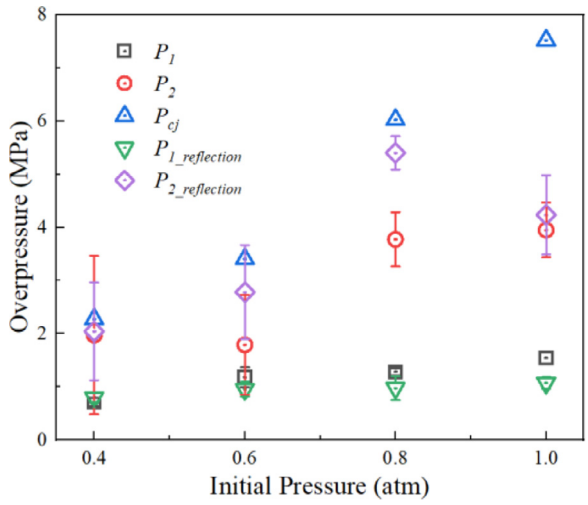

Fig. 6. The peak overpressure profile measured by the two pressure sensors installed in middle (P_1) and end (P_2) positions of tube ($P_{1\_reflection}$ and $P_{2\_reflection}$ refer to the peak overpressure of reflection wave measured by P_1 and P_2, respectively.).

the supersonic state rapidly within a relatively short distance. In Fig. 7(a), the flame firstly accelerates to the maximum value rapidly within a relatively short distance and then propagates over some distance with the maximum velocity before decelerating to travel around $1/2V_{cj}$ or the sound speed in products. Here, the maximum velocity has not reached the theoretical C-J detonation velocity (V_{cj}) at 0.4 atm and 77 K, indicating that detonation does not reach and the flame is still in the fast deflagration stage. This is consistent with the measured pressure and the decoupled state of flame and shock waves.

The $1/2V_{cj}$ regime has been observed in the failure or re-establishment of detonation in many studies. For example, after flame propagates into a solid walled section from a porous walled section, the flame maintains around the $1/2V_{cj}$ before accelerating to an overdriven detonation [16]. Furthermore, the critical deflagration is considered as a C-J deflagration which consists of a leading shock wave followed by an extended turbulent reaction zone and propagates at the $1/2V_{cj}$ for a certain duration prior to the onset of detonation [17,18].

From Fig. 7(b) and 7(c), it is seen that the flame velocity fluctuates back and forth between the C-J deflagration state and the C-J detonation state after accelerating to the first maximum value. In Fig. 7(d), flame accelerates to V_{cj}, then fails to remain stable and decays to $1/2V_{cj}$. The fact that there is a critical deflagration prior to the onset of detonation, is also consistent with previous studies [17,18].

Please cite this article as: X. Shen, W. Fu, W. Liang et al., Strong flame acceleration and detonation limit of hydrogen-oxygen mixture at cryogenic temperatures, Proceedings of the Combustion Institute, https://doi.org/10.1016/j.proci.2022.07.005

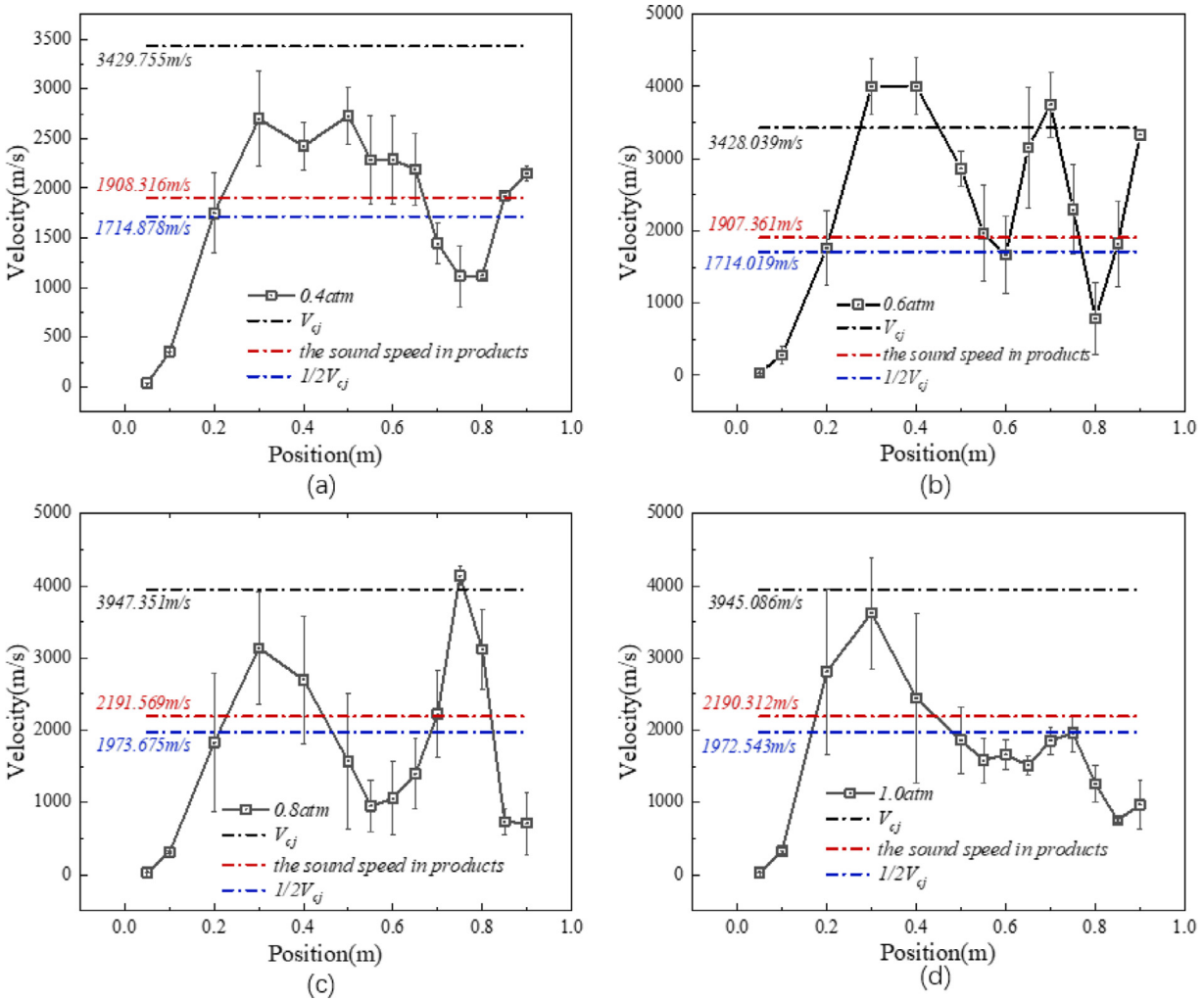

Fig. 7. The flame propagation velocity as function of position at different initial pressures and 77 K.

Please cite this article as: X. Shen, W. Fu, W. Liang et al., Strong flame acceleration and detonation limit of hydrogen-oxygen mixture at cryogenic temperatures, Proceedings of the Combustion Institute, https://doi.org/10.1016/j.proci.2022.07.005

4.3. Strong flame acceleration (FA)

It is seen from Fig. 7(a)−7(d) that the flame starts to accelerate to the maximum velocity rapidly within a relatively short distance for the considered cases. In deflagration, the thermal diffusion from hot combustion products to unburned gas ahead of flame drives the flame propagation. The cold unburned gas becomes the hot combustion products through the flame which correspondingly forms the temperature gradient. Subsequently, thermal diffusion caused by temperature gradient can preheat the upstream unburned gas. Meanwhile, expansion of the hot combustion products promotes the propagation of flame into unburned gas and the movement of unburned gas towards flame. There is a tendency of increasing for both maximum temperature gradient and expansion ratio with decreasing initial temperature. The larger temperature gradient strengthens the thermal diffusion to preheat the unburned gas and the larger expansion ratio enhances the movement of the flame toward unburned gas.

Dorofeev et al. [19] confirmed that sufficiently large expansion ratio was a necessary condition for strong FA. They proposed that the potential ability of strong FA or weak FA for a given mixture could be estimated by the expansion ratio and Zeldovich number (β). Subsequently, Dorofeev [20] analyzed the critical condition of quenching/re-ignition of the largest mixed eddies with Eq. (2).

$$\frac{\sigma^2\beta^2(\beta/2-1)^n e^{1-\beta/2}}{6Le_{eff}{}^n\Gamma_{n+1}\mu}=1 \tag{2}$$

where $\mu\approx 20$ is a constant, σ is the expansion ratio, β is the Zeldovich number, Le_{eff} is the effective Lewis number, $n=n_F+n_O$ is the overall reaction order and $\Gamma_{n+1}\equiv\int_0^\infty \xi^n e^{-\xi}d\xi$ is the Gamma function. The overall reaction order can be calculated by Eq. (3) [21]:

$$n=2\left\{\frac{\partial[\ln \rho_u S_L]}{\partial[\ln P]}\right\}_{T_b} \tag{3}$$

FA is closely associated with the interaction between flame and the turbulence generated in the flow ahead of the flame. The positive feedback for FA will be generated as the result of this interaction through increase of the flame surface, flow speed and turbulence intensity at the early stage. However, as the flame propagates forward, the largest mixed products/reactants pockets will form in the flow ahead of the flame at a certain stage. When the quenching effect of the largest mixed pockets dominates corresponding to the left-hand side of Eq. (2) less than unity, the overall energy release rate will be suppressed, and the positive feedback will be destroyed. If the re-ignition effect of the largest mixed pockets dominates corresponding to the left-hand side of Eq. (2) greater than unity, mixing of products and reactants by turbulence will not affect the energy release rate and the positive feedback will be sustained. Based on Eq. (2), the potential ability of forming strong FA or weak FA for a given mixture can be evaluated. Strong FA leads to fast supersonic combustion flame regime while weak FA causes slow combustion flame regime.

Table 4
The calculations at different initial pressures with Eq. (2).

P_0 (atm)	n	298.15 K	77 K
0.4	2.289	2.578	32.026
0.6	2.245	2.656	32.906
0.8	2.211	2.794	34.052
1.0	2.187	2.837	34.486

The calculated results with the left-hand side of Eq. (2) at 298.15 K and 77 K are shown in Table 4. At the considered conditions, the left-hand side of Eq. (2) are all greater than unity, indicating that positive feedback generated through the interaction between flame and turbulence in the flow of unburned gas will not be destroyed by mixed products/reactants eddies. And the positive feedback will promote flame to form strong FA. The comparison in Table 4 also shows that the results for 77 K are greater than those for 298.15 K, which demonstrates greater potential of forming strong FA at lower temperature. Furthermore, present experimental results illustrate that strong FA occurs in line with the above analysis, indicating that Eq. (2) is applicable to cryogenic temperature.

Besides expansion ratio (σ) and Zeldovich number (β), the transverse size of the tube should be at least two orders of magnitude larger than the laminar flame thickness for strong FA [22]. In this study, the inner diameter of the experimental tube (D) is 2 cm which is at least two orders of magnitude larger than the thermal thickness of laminar flame (0.186 mm) at 0.4 atm and 77 K. And as initial pressure increases, the thermal thickness of laminar flame decreases. Therefore, the requirement of tube diameter for strong FA is satisfied.

After the requirements of mixture properties and tube diameter for strong FA are all satisfied, the sufficient distance for the slow laminar flame to accelerate rapidly to high supersonic deflagration is essential. In the study of Dorofeev [23], the run-up distance to supersonic flame for hydrogens mixtures in relatively smooth tubes is investigated. A simple model to predict the run-up distance where the flame speed reaches the sound speed in the combustion products (X_s) is,

$$\frac{X_s}{D}=\frac{\psi}{C}\left[\frac{1}{\kappa}\ln\left(\psi\frac{D}{d}\right)+K\right] \tag{4}$$

where D/d can be calculated by the blockage ratio (BR): $D/d=2/(1-(1-BR)^{1/2})$, D is the inner diameter of tube. The parameters κ, K and C are con-

Please cite this article as: X. Shen, W. Fu, W. Liang et al., Strong flame acceleration and detonation limit of hydrogen-oxygen mixture at cryogenic temperatures, Proceedings of the Combustion Institute, https://doi.org/10.1016/j.proci.2022.07.005

Table 5
The calculation results of run-up distance to supersonic flame (X_s) at 77 K and 298.15 K.

P_0 (atm)	298.15 K	77 K	Present study
0.4	1.217	0.493	0.2–0.3
0.6	1.068	0.428	0.2–0.3
0.8	0.977	0.424	0.2–0.3
1.0	0.915	0.402	0.15–0.2

stants (independent of mixture composition) taken to be: $\kappa = 0.4$, $K = 5.5$ and $C = 0.2$ [24]. ψ can be calculated by Eq. (5).

$$\psi = \left[\frac{a_p}{\eta(\sigma - 1)^2 S_L} \left(\frac{\delta}{D} \right)^{1/3} \right]^{1/(2m+7/3)} \tag{5}$$

where m and η are unknown parameters which are determined using an appropriate set of experimental data: $m = -0.18$ and $\eta = 2.1$. a_p is the sound speed in combustion products, m/s. In the study of Dorofeev [23], the model was shown to estimate the experimental data with an accuracy of prediction for the run-up distances of about ±25%.

Table 5 lists the calculation results of run-up distance to supersonic flame (X_s) at 77 K. In this study, the experimental tube is smooth and when using Eqs. (4) and (5), the BR is assumed to be 0.01. It is seen from Fig. 7 that the flame accelerates to supersonic in the position range of 0.2–0.3 m and 0.15–0.2 m in the case of 0.4 atm-0.8 atm and 1.0 atm, respectively. It is seen from Table 5 that X_s at 298.15 K is at least two times larger than at 77 K which shows that lower temperature reduces X_s.

In this study, lower temperature causes larger density of unburned gas (ρ_u) for the same initial pressure, making the initially unburned mixture close to the liquid phase. Due to the density of combustion products (ρ_b) is not sensitive to the initial temperature, the larger density of unburned gas (ρ_u) causes significantly larger expansion ratio (σ). In addition to the expansion ratio, thermal diffusion is also strengthened by the larger temperature gradient and the maximum temperature gradient increases as the initial temperature decreases. The unburned gas can be preheated by thermal diffusion from hot combustion products.

4.4. Detonation limits

It is seen from Fig. 7 that there is a periodic fluctuation for flame velocity after flame rapidly accelerates to V_{cj} at 0.6–1.0 atm. The periodic failure and re-ignition of detonation is considered as the galloping mode [25]. When detonation limit appears, the galloping mode can be observed in many unstable mixtures [26,29], corresponding to irregular detonation cell structures. However, with increasing amount of inert gas, the stability of mixtures gets strengthen which shows a regular detonation cell structure. In these mixtures, the galloping mode cannot be observed near the limit condition [26,29]. When the initial pressure is below the limit condition, the fast flame mode, which flame propagates with $1/2V_{cj}$, is observed [27]. Due to the irregularity of the detonation cell structure for unstable mixtures, the galloping mode generally is considered as limiting mode. The limit of detonation is determined by the balance between the rate of heat loss to tube wall and the rate of heat production by chemical reactions. Lower initial pressure shortens the rate of heat production which leads to the detonation limit [27]. As the limit is approached, the larger velocity fluctuation appears before failure of detonation occurs [28].

Radulescu [29,30] first links the stability parameter χ with the cellular structure regularity of detonation and the irregular detonation cell structure can be observed in condition of $\chi > 10$, where the χ parameter is defined as the ratio of the induction time (t_i) to the reaction time (t_e) multiplies the activation energy normalized by local temperature (T_{vn}) behind detonation shock wave ($\frac{E_a}{RT_{vn}}$).

$$\chi = \frac{t_i}{t_e} \frac{E_a}{RT_{vn}} \tag{6}$$

The induction time (t_i) is defined as the delay to the point of maximum exothermicity ($\dot{\sigma}_{max}$) from the shock wave, and the reaction time (t_e) is defined as the inverse of the maximum exothermicity ($\dot{\sigma}_{max}$). The exothermicity ($\dot{\sigma}$) is expressed as Eq. (7):

$$\dot{\sigma} = (\gamma - 1) \frac{Q}{c_{vn}^2} \frac{d\lambda}{dt} \tag{7}$$

where γ is the specific heat ratio, Q is the chemical reaction heat release, J/kg, c_{vn} is the sound speed behind the shock wave, m/s and λ is the reaction progress variable. The induction time is closely associated with the initial temperature which can be described as the form of $t_i \propto exp(\frac{E_a}{RT_{vn}})$. Thus, the activation energy can be obtained by calculating the induction times at two different temperatures behind the shock wave at the velocity of $(100 \pm 1)\% Vcj$, respectively. It can be expressed as Eq. (8):

$$\frac{E_a}{RT_{vn}} = \frac{1}{T_{vn}} \left(\frac{\ln t_1 - \ln t_2}{1/T_1 - 1/T_2} \right) \tag{8}$$

Induction time (t_i) is the time scale for the gradient of reactivity to be set by the shock and a larger ratio of the induction time to reaction time means sufficient time for the pressure wave to accelerate. The parameter χ is an indicator reflecting the stability of self-propagating detonation waves [30,31]. The calculated χ parameter is listed in Table 6.

According to references [25–28], the periodic failure and re-ignition of detonation is considered as the galloping mode, which can be observed in unstable mixtures near the limit condition and is

Please cite this article as: X. Shen, W. Fu, W. Liang et al., Strong flame acceleration and detonation limit of hydrogen-oxygen mixture at cryogenic temperatures, Proceedings of the Combustion Institute, https://doi.org/10.1016/j.proci.2022.07.005

Table 6
The calculation results of χ parameter at 77 K.

P_0 (atm)	t_i/t_e	E_a/RT_{vn}	χ
0.4	17.479	13.330	232.996
0.6	22.253	16.173	359.897
0.8	26.198	15.821	414.491
1.0	28.772	15.403	443.170

generally considered as the limiting mode. The measured flame velocity curves of 0.6–1.0 atm in Fig. 7 are consistent with the features of the galloping mode, which means the detonation limit is approached. It is seen from Table 6 that the χ parameter is much larger than 10 at different initial pressures which shows the unstable mixture in present study. By further decreasing the initial pressure, detonation cannot be formed and the fast flame mode, in which flame propagates with $1/2V_{cj}$, is observed at 0.4 atm. The result that flame propagates with about $1/2V_{cj}$ in fast flame mode is consistent with previous study[27]. It is noted that due to the limit of the tube length, the galloping mode may be mistakenly treated as a fast flame like Fig. 7(d) at 1.0 atm [25].

5. Conclusion

Strong flame acceleration (FA), fast flame and the subsequent galloping detonation of hydrogen-oxygen mixtures in tube are investigated with different initial pressures at cryogenic temperature of 77 K. The conclusions are as follows:

(1) Both the 1st and 2nd shock waves are captured in the experiments.
(2) During flame propagation, the 1st and 2nd shock waves eventually coalesce into a stronger precursor shock. However, both are decoupled from the flame in all the considered cases, indicating absence of stable detonation.
(3) Strong flame acceleration is observed in all cases, which is consistent with the prediction by the expansion ratio and Zeldovich number.
(4) All the flames in this work accelerate drastically to reach the C-J deflagration state. But at 0.4 atm, only fast flame is formed, while at higher initial pressures, the flame further accelerates to a galloping detonation.
(5) The stability parameter χ is a proper indicator of near-limit detonation in unstable mixture presenting a galloping mode of oscillation.

Declaration of Competing Interest

The authors declare that they have no known competing financial interests or personal relationships that could have appeared to influence the work reported in this paper.

Acknowledgements

This work was supported by the National Natural Science Foundation of China (Grant No. 22078095 and 51604121) and the Shanghai Science and Technology Committee (Grant No. 20dz1200903 and 21QC1400400). This work was also supported by the Individual Fellowship Scheme of the European Union's Horizon 2020 Marie Skłodowska-Curie Actions (Grant No. 891173, HYGAS).

References

[1] G.A. Karim, I. Wierzba, S. Boon, *Cryogenics (Guildf)* 24 (6) (1984) 305–308.
[2] G. Cui, S. Wang, J. Liu, Z. Bi, Z. Li, *Fuel* 234 (2018) 886–893.
[3] P.P. Panda, E.S. Hecht, *Int. J. Hydrogen Energy* 42 (1) (2017) 775–785.
[4] J.E. Hall, P. Hooker, D. Willoughby, *Int. J. Hydrogen Energy* 39 (35) (2014) 20547–20553.
[5] E.S. Hecht, B.R. Chowdhury, *Int. J. Hydrogen Energy* 46 (23) (2021) 12320–12328.
[6] Z. Ren, J.X. Wen, Flame characteristics of ignited under-expanded cryogenic hydrogen jets, *Int. Conf. on Hydrogen Safety*, 2021.
[7] D.M.C. Cirrone, D. Makarov, V. Molkov, *Int. J. Hydrogen Energy* 44 (17) (2019) 8886–8892.
[8] M. Kuznetsov, A. Denkevits, A. Veser, A. Friedrich, G. Necker, T. Jordan, Shock tube experiments on flame propagation regimes and critical conditions for flame acceleration and detonation transition for hydrogen-air mixtures at cryogenic temperatures, *Int. Conf. on Hydrogen Safety*, 2021.
[9] R.J. Kee, J.F. Grcar, M.D. Smooke, J.A. Miller, E. Meeks, *[Tech. Rep.] SAND (SAND85-8249)* (1985).
[10] M.P. Burke, M. Chaos, Y. Ju, F.L. Dryer, S.J. Klippenstein, *Int. J. Chem. Kinet.* 44 (7) (2012) 444–474.
[11] G.S. Soave, *Chem. Eng. Sci.* 34 (2) (1979) 225–229.
[12] M. Kellenberger, G. Ciccarelli, *Combust. Flame* 191 (2018) 195–209.
[13] J. Cheng, B. Zhang, H. Liu, F. Wang, *Fuel* 283 (2021).
[14] L.F.M. Gárzon Lama, L. Pizzuti, J. Sotton, C.A. Martins, *Fuel* 287 (2021).
[15] Q. Zhou, C.S. Cheung, C.W. Leung, X. Li, Z. Huang, *Fuel* 248 (2019) 8–15.
[16] M.I. Radulescu, J.H.S. Lee, *Combust. Flame* 131 (1) (2002) 29–46.
[17] Y.J. Zhu, J. Chao, J.H.S. Lee, *Proc. Combust. Inst.* 31 (2007) 2455–2462.
[18] R.S. Chue, J.F. Clarke, J.H. Lee, *Proc. R. Soc. Lond A* 441 (1993) (1913) 607–623.
[19] S.B. Dorofeev, M.S. Kuznetsov, V.I. Alekseev, A.A. Efimenko, W. Breitung, *J. Loss Prev. Process Ind.* 14 (6) (2001) 583–589.

Please cite this article as: X. Shen, W. Fu, W. Liang et al., Strong flame acceleration and detonation limit of hydrogen-oxygen mixture at cryogenic temperatures, Proceedings of the Combustion Institute, https://doi.org/10.1016/j.proci.2022.07.005

[20] S. Dorofeev, *Proc. Combust. Inst.* 31 (2007) 2371–2379.
[21] F.N. Egolfopoulos, C.K. Law, *Combust. Flame* 80 (1) (1990) 7–16.
[22] G. Ciccarelli, S. Dorofeev, *Prog. Energy Combust. Sci.* 34 (4) (2008) 499–550.
[23] S.B. Dorofeev, *Int. J. Hydrogen Energy* 34 (14) (2009) 5832–5837.
[24] M. Kuznetsov, V. Alekseev, I. Matsukov, S. Dorofeev, *Shock waves* 14 (3) (2005) 205–215.
[25] J. Lee, G. Dupré, R. Knystautas, J. Lee, *Shock Waves* 5 (3) (1995) 175–181.
[26] F. Haloua, M. Brouillette, V. Lienhart, G. Dupré, *Combust. Flame* 122 (4) (2000) 422–438.
[27] S. Kitano, M. Fukao, A. Susa, N. Tsuboi, A. Hayashi, M. Koshi, *Proc. Combust. Inst.* 32 (2009) 2355–2362.
[28] J.H. Lee, A. Jesuthasan, H.D. Ng, *Proc. Combust. Inst.* 34 (2013) 1957–1963.
[29] M.I. Radulescu, *The propagation and failure mechanism of gaseous detonations: experiments in porous-walled tubes, Ph.D. Thesis*, McGill University, 2003.
[30] J. Tang, M.I. Radulescu, *Proc. Combust. Inst.* 34 (2) (2013) 2035–2041.
[31] M. Radulescu, G. Sharpe, D. Bradley, in: ISFEH7 Proceedings of the Seventh International Seminar, 2013, pp. 617–626.
[32] J. Cheng, B. Zhang, H. Liu, F. Wang, *Aerospace Science and Technology* 106 (2020).
[33] D. Lapalme, F. Halter, C. Mounaïm-Rousselle, P. Seers, *Combustion and Flame* 193 (2018).

Please cite this article as: X. Shen, W. Fu, W. Liang et al., Strong flame acceleration and detonation limit of hydrogen-oxygen mixture at cryogenic temperatures, Proceedings of the Combustion Institute, https://doi.org/10.1016/j.proci.2022.07.005